Available online at www.sciencedirect.com
SCIENCE DIRECT®
Coordination Chemistry Reviews 248 (2004) 853–866
COORDINATION CHEMISTRY REVIEWS
www.elsevier.com/locate/ccr

Review

Conformational and linkage isomerizations for dihapto-coordinated arenes and aromatic heterocycles: controlling the stereochemistry of ligand transformations

W. Dean Harman*

Department of Chemistry, University of Virginia, McCormick Road, Charlottesville, VA 22904-4319, USA

Received 22 December 2003; accepted 30 March 2004

Available online 19 May 2004

Contents

Abstract

Arenes and aromatic heterocycles have cyclic skeletons made up completely of unsaturated carbons. Through their dihapto coordination to a transition metal, controlled addition reactions can be accomplished with good stereocontrol, relative to the position of the metal. The metal can readily undergo inter- and intrafacial linkage isomerizations in these complexes. By controlling these processes using chiral auxiliaries on the arene, stereogenic metal centers, or solid-state induced control of kinetically unstable stereoisomers (SICKUS), enantio-enriched organic compounds can be realized from this methodology. This work outlines what is known about conformational and linkage isomerizations in dihapto-coordinated aromatic complexes, and demonstrates their relevance to organic synthesis.

Keywords: Isomerization; Osmium; Rhenium; Tungsten; Molybdenum; Arene; Dearomatization

1. Introduction

For over four decades, organometallic chemists have exploited the ability of transition metals to promote otherwise inaccessible reactions of arenes [1–4]. Most commonly, this chemistry arises from a complex in which the arene is hexahapto-coordinated to an electron-deficient metal atom. For example, in the case of (arene)$Cr(CO)_3$, the effect of metal coordination is considered to be comparable to a nitro group attached to the ring. As a consequence, the arene is readily attacked by nucleophiles to generate stable cyclohexadienyl anion complexes [2]. Depending on work-up

* Tel.: +1-434-924-3060; fax: +1-434-924-3710.
E-mail address: wdh5z@virginia.edu (W.D. Harman).

0010-8545/$ – see front matter © 2004 Elsevier B.V. All rights reserved.
doi:10.1016/j.ccr.2004.03.013

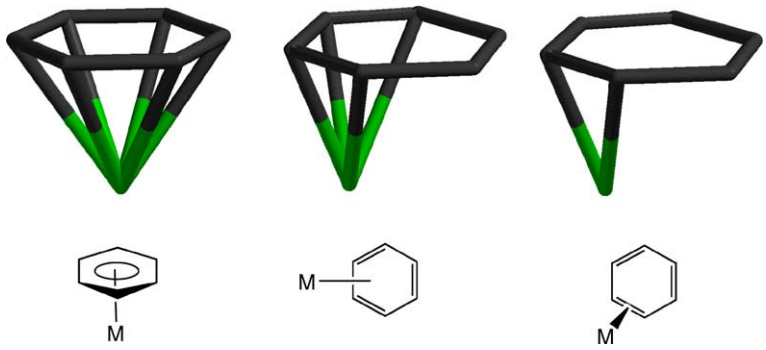

Fig. 1. Common coordination modes for arenes.

conditions, either substituted cyclohexadienes or arenes can be recovered, free of the metal. While other coordination modes for arenes have been known for many years (Fig. 1) [5], little was known about the organic chemistry of these types of arene ligands prior to the late 1980s.

In 1985, while under the guidance of Henry Taube, I was asked to investigate the coordination chemistry of the seemingly pedestrian complex fragment $\{Os(NH_3)_5\}^{2+}$. The development by Lay et al. of a high-yield route to $Os(NH_3)_5(OTf)_3$ not only opened the doors for the exploration of pentaammineosmium(III) chemistry [6], but also provided a new window into the chemistry of its divalent cousin. My task was simply to reduce the osmium(III) in a solvent that would not interfere with coordination of a designated ligand. Soon after these conditions were discovered (DMA/Mg°) [7,8], it became apparent that the chemistry of pentaammineosmium(II) was going to be dramatically different from the ruthenium analog [9]. Most notably, the pentaammineosmium(II) fragment displayed a remarkable ability to bind arenes across two carbons (i.e., η^2). In contrast to the silver and copper adducts of arenes that have been known for over half a century [10,11], the osmium arene complexes were found to be substitution-inert, the ligand being replaced by solvent or other ligand only after a matter of hours at 20 °C [8].

This uncommon binding mode of arenes would ultimately be responsible for a wide range of new organic transformations that take advantage of the ability of the metal to break the aromatic stabilization of the ring [12]. In contrast to the well established hexahapto-arene chemistry, the osmium arene complexes are prone to undergo electrophilic addition reactions, the metal acting as an electron-donor. Just as Cr(0), for example, has the ability to stabilize the cyclohexadienyl anion resulting from addition of a nucleophile, so does the osmium stabilize the cyclohexadienyl cation resulting from addition of an electrophile.[1] The resulting arenium

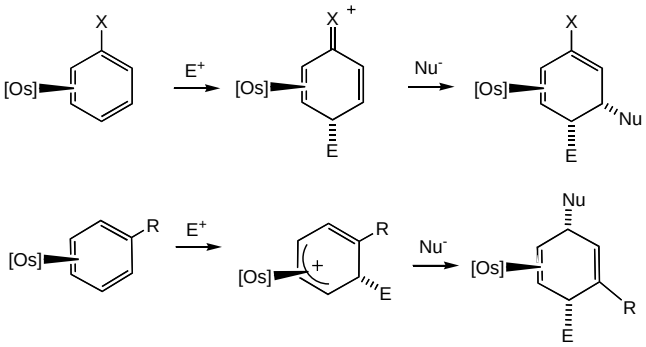

Fig. 2. Tandem addition reactions with η^2-arene complexes (E = electrophile, Nu = nucleophile).

ion can then be combined with a nucleophile to effect an overall tandem addition sequence to the arene (Fig. 2) [12].

For dihapto-coordinated arene complexes, both the electrophile and the nucleophile add to the face of the arene *opposite to* metal coordination [8]. in the process, two new stereocenters are formed from the ring carbons, usually with excellent stereocontrol, relative to the position of the metal (see Fig. 2). Thus, if the position of metal coordination can be controlled, then the regio- and stereochemistry of the organic product can be as well. In order to achieve this goal we needed to become familiar with the various dynamic processes by which the metal of a dihapto-coordinated arene can adjust its binding. The following account describes these coordination (linkage) isomerizations, and how they can be used to control the regio- and stereochemistry of organic transformations.

2. Linkage isomerizations of pentaammineosmium(II)

2.1. η^2-Arene complexes

The parent osmium(II)–arene complex, $[Os(NH_3)_5(\eta$-benzene$)]^{2+}$ (**1**), shows a single broad peak at 6.45 ppm in its ^{1}H NMR spectrum recorded at 20 °C, corresponding to the six ring protons [13]. Lowering the temperature to −87 °C causes this broad feature to split into three well

[1] Note that one could also describe this reaction as the two-electron oxidation of the metal accompanied by the formation of an organic anion. However, the chemistry of the ligand most closely resembles an arenium cation.

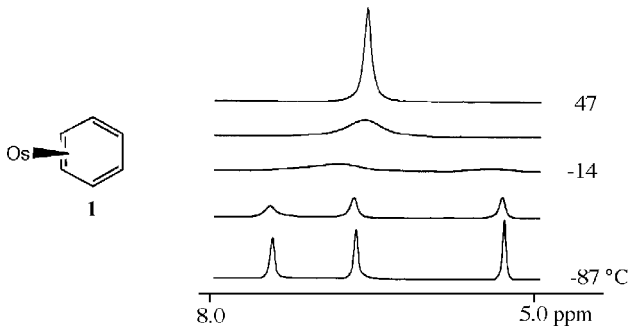

Fig. 3. Variable temperature ^{1}H NMR spectra (400 MHz) for $[Os(NH_3)_5(\eta^2\text{-benzene})]^{2+}$ (**1**).

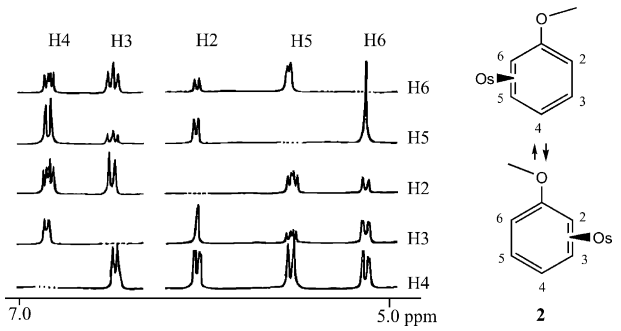

Fig. 5. Selective proton decoupled ^{1}H NMR spectra of anisole complex **2** (Os = $[Os(NH_3)_5]^{2+}$).

resolved peaks ranging from 5.22 to 7.25 ppm (Fig. 3). Using band shape analysis, a rate of $1 \times 10^4\ s^{-1}$ was determined at 20 °C for isomerization, corresponding to a free energy of activation of 11.8 kcal/mol at this temperature [14]. This barrier is considerably higher than what had been reported prior to the discovery of **1** [15]. The mechanism responsible for averaging the ring proton signals was thought to be an intrafacial linkage isomerization (*ring walk*), in which the metal moves from one pair of carbons to the next by either an η^3 or η^1 intermediate (Fig. 4). Others have speculated that the process involves a σ complex or phenyl hydride intermediate [16–18]. While the latter mechanism would also allow the metal to change the face that was coordinated (an interfacial linkage isomerization), such a *face-flip* would go undetected in the case of a benzene ligand, due to its high symmetry (see Fig. 4).

The addition of a methoxy group to the arene changes the situation profoundly [14]. The ^{1}H NMR spectrum for the anisole complex $[Os(NH_3)_5(anisole)]^{2+}$ (**2**) shows five fully resolved ring proton signals at ambient temperature (Fig. 5), corresponding to a complex in which the anisole is bound selectively across C5 and C6. In this position, the metal, by disrupting cross-conjugation, enhances the π interaction of the methoxy group and the uncoordinated portion of the arene ring. Such an interaction is supported with DFT calculations [19], as well as NMR data [14]. The observance of spin saturation exchange indicates that the metal is still undergoing a fluxional process at 20 °C, but the event is clearly much slower than for the parent benzene complex. Fig. 5 shows data for a series of spectra recorded with one of the five ring proton resonances irradiated. The loss of intensity to the complementary signal is readily apparent. For example, irradiation of the peak at 5.06 ppm (H6) corresponding to the bound *ortho* proton results in a decrease in the peak at 5.72 ppm (H2), corresponding to the unbound signal [14]. Although these correlations indicate that there is conversion between the two enantiomers shown in Fig. 5, it does not indicate whether this interconversion occurs via a inter- or intrafacial linkage isomerization (see Fig. 4).

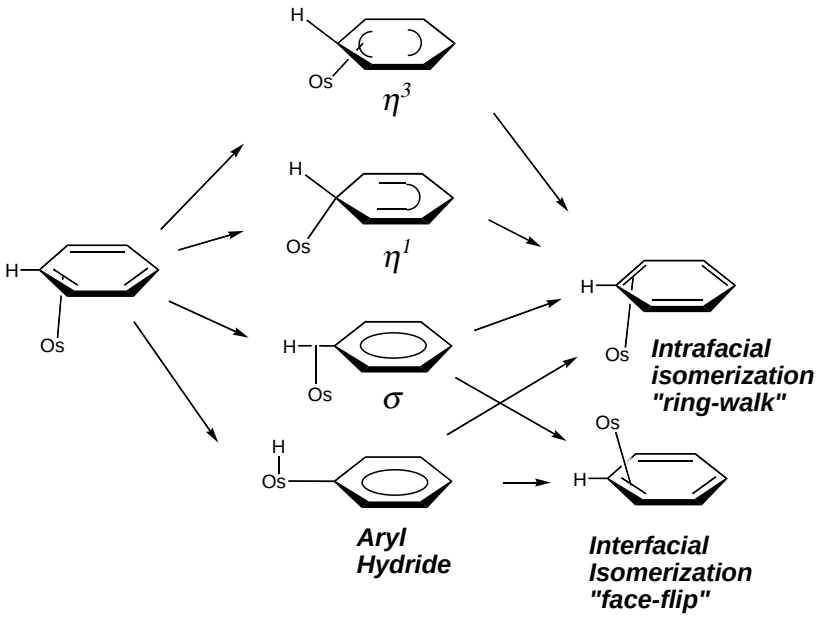

Fig. 4. Intra- and interfacial isomerization mechanisms (Os = $[Os(NH_3)_5]^{2+}$).

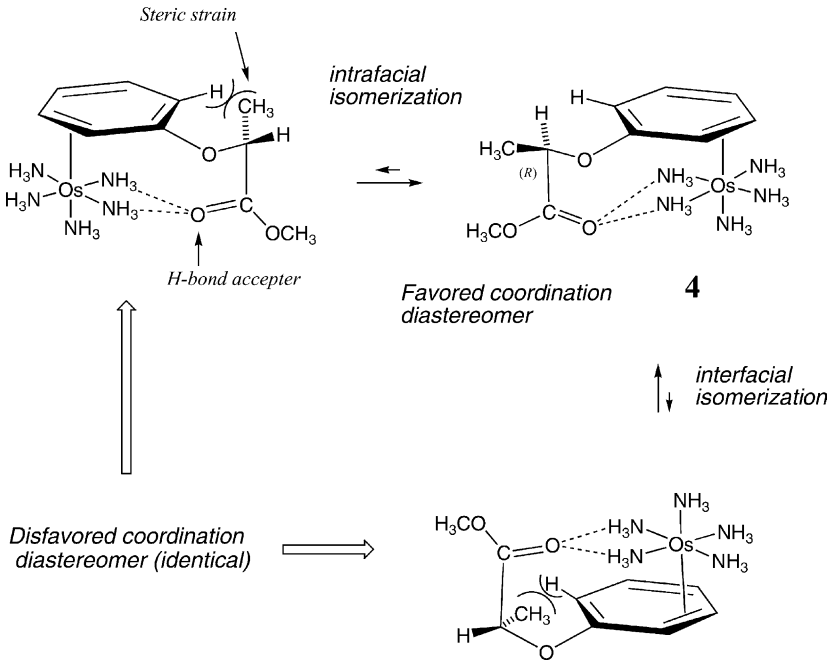

Fig. 6. Coordination diastereomers for the lactate-derived anisole complex (**4**).

In order to resolve this issue, several modified anisoles derived from lactic acid were prepared and complexed to osmium [20]. The complex $Os(NH_3)_5(PhOCH(CH_3)CH_2OCH_3)$ (**3**), with its remote stereogenic center, affords two coordination diastereomers (3:1) [21]. In contrast, the ester derivative $Os(NH_3)_5(PhOCH(CH_3)COOCH_3)$ (**4**) is highly selective, showing only the coordination diastereomer indicated in Fig. 6.

Although spin saturation exchange data for the anisole complex **2** indicated the presence of linkage isomerization, these data could not differentiate between inter- and intrafacial isomerizations. The answer as to which mechanism is operative is found partially in a spin saturation study of **3**, where both coordination diastereomers are detectable in the proton NMR spectrum. In this experiment (Fig. 7), irradiation of the bound ortho proton of one diastereomer was correlated with the unbound ortho proton on the *other* coordination diastereomer (H6′ exchanges with H2). This observation indicates that the most rapid mechanism for interconversion of diastereomers is an intrafacial linkage isomerization (ring-walk; Fig. 8) [21]. Note that a face-flip mechanism cannot be excluded, but if the face-flip process is operative (where H6′ exchanges with H6), the specific rate would be too slow, compared to the intrafacial process, to be detected.

The spin saturation data (Fig. 7) are consistent with a rate approximately equal to that observed for anisole, with

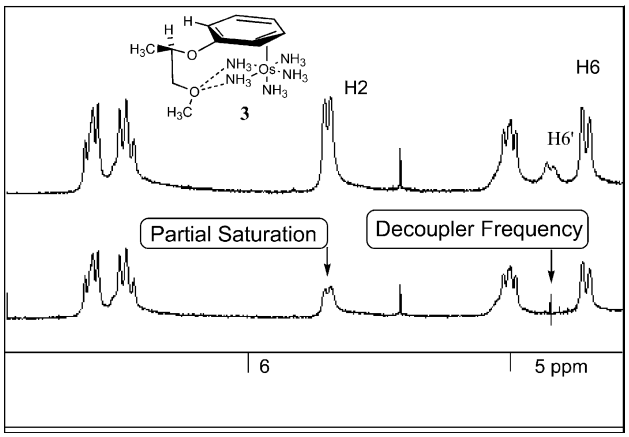

Fig. 7. Spin saturation data for the 1-methoxy-2-phenoxypropane complex **3**.

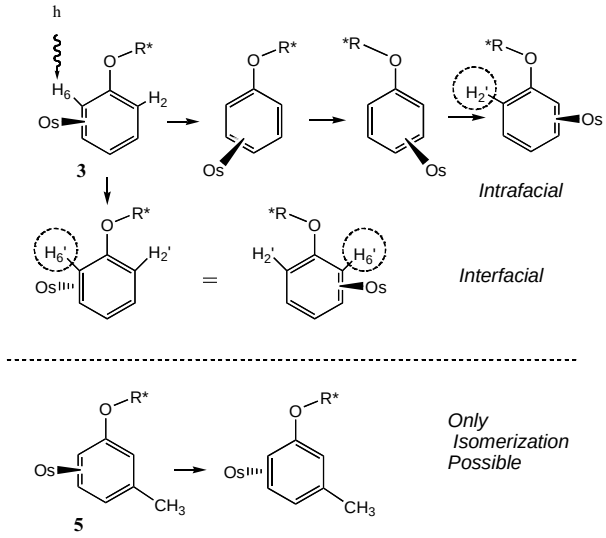

Fig. 8. Intrafacial (**3**) and interfacial (**5**) isomerization for η^2-anisole complexes.

both anisole complexes showing rates of isomerization much slower than that seen for the benzene complex. This lower rate of intrafacial isomerization for the anisole complexes can be attributed to higher energy of the 3,4-η^2 or 1,2-η^2 intermediates, which presumably lie along the reaction coordinate of 2,3-η^2 to 5,6-η^2 isomerization (Fig. 8).

We also investigated an anisole complex with both a chiral auxiliary and a methyl group at the 3-position (**5**; see Fig. 8). This complex cannot undergo an intrafacial linkage isomerization without creating a constitutional isomer. Thus, if an intrafacial isomerization is the only dynamic process operative for these complexes, then there should be no mechanism available to interconvert coordination diastereomers of **5**. Yet, when 1-methoxy-2-(3-methylphenoxy)propane is complexed with the pentaammineosmium(II) fragment, the ratio of coordination diastereomers exactly equals that observed for **3** (complex **5** less the 3-methyl group) at equilibrium. With no reason to assume that the ratio of arene binding rate constants for **5** should equal that of the equilibrium ratio for **3**, we hypothesized that the coordination isomer ratio of **5** is also under thermodynamic control, and further, that an *interfacial* isomerization could be operative on a time scale not too different from the intrafacial isomerization mechanism. An interfacial isomerization for a rhenium alkene complex was reported by Peng and Gladysz [22], and similar isomerizations have recently been documented for Mo and Re in our laboratories (vide infra).

Polycyclic aromatic hydrocarbons are readily coordinated by pentaammineosmium(II) [23]. In comparison to the benzene analog (**1**) the naphthalene complex **6** shows much slower rates of isomerization. For **6**, two isomerization processes have been characterized. The more rapid of the two is the intrafacial isomerization analogous to that observed with benzene, which has a specific rate of $10^{-3} < k < 1$ (20 °C). At a much slower rate, an inter-ring isomerization also takes place. This process, which occurs over a period of many days at 20 °C ($k = 2 \times 10^{-6}\,s^{-1}$), was identified utilizing 1-methylnaphthalene [23] in order to differentiate between the two rings. As with anisole, the slower intrafacial isomerization for the naphthalene complex relative to that of benzene, can be attributed to the higher energy intermediate the metal must pass through (Fig. 9).

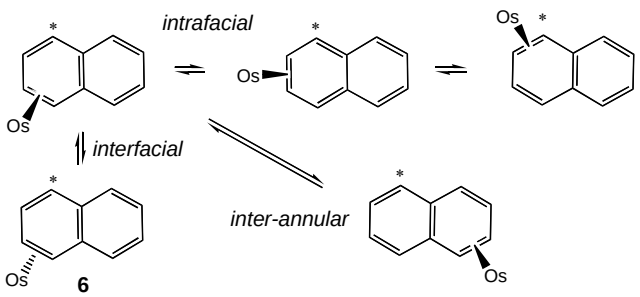

Fig. 9. Possible coordination isomerizations for an η^2-naphthalene complex (**6**).

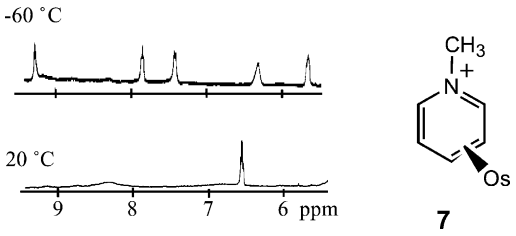

Fig. 10. Variable temperature NMR data (400 MHz) for pyridinium complex **7**.

2.2. η^2-Aromatic heterocycle complexes

Dynamic processes similar to those observed for η^2-arene complexes of osmium are operative in heterocyclic complexes. While pyridines typically afford N-bound complexes with pentaammineosmium(II), *N*-methylpyridinium salts are readily η^2-coordinated. In the complex $[Os(NH_3)_5(\eta^2\text{-Mepy})]^{3+}$ the metal preferentially binds across C4 and C5, but as with the benzene analog, the room temperature ^{1}H NMR spectrum is severely broadened [24]. Reducing the temperature to −60 °C reveals a set of five signals corresponding to the 4,5-η^2 species (Fig. 10).

Again, one could consider both inter- and intrafacial isomerization processes responsible for the broadening observed in the room temperature proton NMR spectrum. At the time this work was done, the interfacial mechanism was not considered, and thus, no experimental data distinguishing the two processes are available. However, indirectly relevant is the observation of a slow decomposition of **7** to form a C4-bound isomer (**8**), the result of oxidative addition followed by proton loss (Fig. 11) [24].

Pyrroles, furans, and thiophenes all form stable complexes with pentaammineosmium(II) in which the heterocycle is dihapto-coordinated [25]. Whereas, the room temperature proton spectrum of furan and thiophene show well resolved resonances indicative of coordination across C4 and C5, the pyrrole analog has a broadened spectrum. Experiments with alkylated furans and thiophenes indicate that linkage isomerizations are operative in these complexes as well, but that they occur at much slower rates [25]. For either the ring-walk or face flip mechanisms outlined above, it is now possible that the purported heteroatom-bound intermediate lies along the reaction coordinate, as shown in Fig. 12.

Three key experiments speak to this mechanistic issue. The first lies in the observation that when methyl groups are

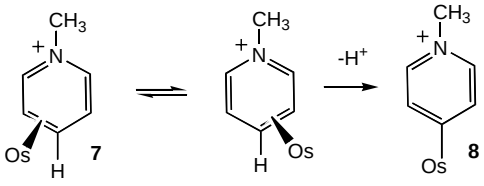

Fig. 11. Intrafacial isomerization and oxidative addition of *N*-methyl pyridinium complex **7**.

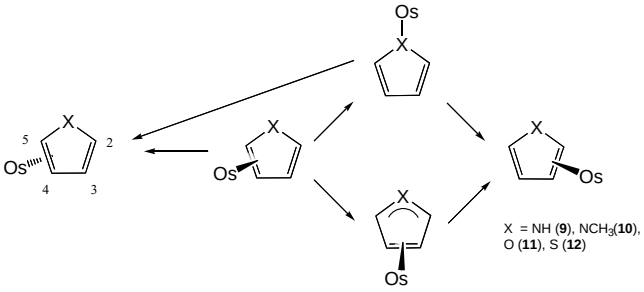

Fig. 12. Possible pathways for an intrafacial isomerization for pyrrole, furan, and thiophene complexes of osmium(II).

present on the pyrrole complex, either at the nitrogen (**10**) or the 2 and 5 positions of the pyrrole (**13**), the fluxional process is greatly accelerated. Whereas, the rate of coordination isomerization is $\ll 70\,s^{-1}$ for the pyrrole complex (**7**), this rate increases to $\sim 10^2\,s^{-1}$ for *N*-methylpyrrole and is $>300\,s^{-1}$ for 2,5-dimethyl pyrrole [26]. A mechanism involving an η^1 complex (bound at the heteroatom) would be expected to have the opposite behavior. Similar qualitative observations have been made with the furan complex (**11**). The second indication of an azomethine ylide intermediate (see Fig. 12) is found in a remarkable reaction of the pyrrole complexes (**9**, **10**, and **13**) with electron-deficient alkenes. In what is best described as a dipolar cycloaddition reaction, 7-azanorbornene complexes (**14**) are formed with rates that mirror that of the isomerization process [27]. We speculate that the presence of the methyl groups increases the equilibrium concentration of the ylide (**13A**), thereby increasing the observed rate of cycloaddition (Fig. 13).

3. Conformational and linkage isomerizations of second generation dearomatization agents

3.1. Rhenium(I) carbonyl complexes

Pentaammineosmium(II) provided a number of novel synthetic transformations with η^2-arenes and aromatic heterocycles [8,12], yet the symmetric nature of this fragment does not allow for the discrimination of enantiofaces of the aromatic ligand. While attachment of a chiral auxiliary to either an anisole [20] or pyrrole [28] ligand has solved this problem in a few special cases (vide infra)

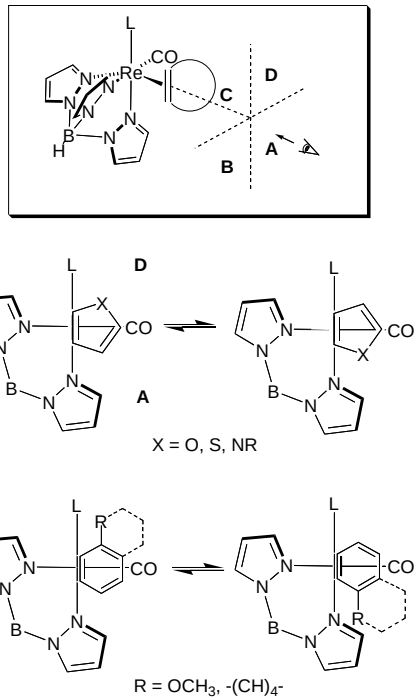

Fig. 14. Quadrant assignments for TpRe(CO)(L) complexes.

[20], a more general approach to this problem was desired. The advent of a series of rhenium carbonyl complexes taking the general form TpRe(CO)(L)(aromatic) (Tp^- = hydridotris(pyrazolyl)borato) offered the possibility of carrying out organic transformations whose stereochemistry was governed by the configuration of the stereogenic metal center [29].

The synthetic approach to these rhenium complexes offered an easy method of adjusting the backbonding ability of the rhenium by varying the nature of the auxiliary ligand, L. Judging from electrochemical and infrared data, as L is adjusted through the series *t*-BuRC < PMe_3 < py > MeIm, the backbonding potential of the metal increases, and this mirrors the stability of the aromatic complex. While naphthalene and furan were readily coordinated by every member in the series, benzenes and pyrroles formed stable complexes only with the most electron-rich complex, where L = MeIm. In all cases, other than the benzene complex, coordination diastereomers were observed. In Table 1, a series of these complexes (**15**–**32**) is listed according to the nature of L. Fig. 14 shows the quadrant assignments indicating the assignment of

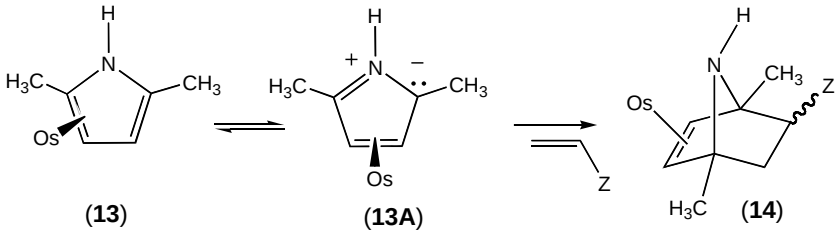

Fig. 13. Dipolar cycloaddition of an osmium(II) pyrrole complex (**13**) and an alkene.

Table 1
Equilibrium constants and diastereoselectivities of $TpRe(CO)(L_D)(\eta^2\text{-}L_{Ar})$ systems

Minor Diastereomer $\underset{k_{-1}}{\overset{k_1}{\rightleftharpoons}}$ Major Diastereomer

$K_{eq}=k_1/k_{-1}$

Compound	K_{eq}	T (K)	Quadrant (R or X of major isomer)
$TpRe(CO)(^t BuNC)(\eta^2$-furan) (**15**)	2.2	273	A
$TpRe(CO)(^t BuNC)(\eta^2$-2-methylfuran) (**16**)	4.9	298	A
$TpRe(CO)(^t BuNC)(\eta^2$-thiophene) (**17**)	4.3[a]	273	A
$TpRe(CO)(^t BuNC)(\eta^2$-naphthalene) (**18**)	1.2	273	D
$TpRe(CO)(^t BuNC)(\eta^2$-2-methoxynaphthalene) (**19**)	1.0	308	A
$TpRe(CO)(^t BuNC)(\eta^2$-1,8-dimethylnaphthalene) (**20**)	1.2	293	D
$TpRe(CO)(PMe_3)(\eta^2$-furan) (**21**)	2.1	323	A
$TpRe(CO)(PMe_3)(\eta^2$-thiophene) (**22**)	1.6[b]	323	A
$TpRe(CO)(PMe_3)(\eta^2$-naphthalene) (**23**)	>19	323	A
$TpRe(CO)(py)(\eta^2$-furan) (**24**)	1.6	323	A
$TpRe(CO)(py)(\eta^2$-thiophene) (**25**)	1.2	323	D
$TpRe(CO)(py)(\eta^2$-naphthalene) (**26**)	3.0	323	D
$TpRe(CO)(MeIm)(\eta^2$-furan) (**27**)	1.4	343	D
$TpRe(CO)(MeIm)(\eta^2$-thiophene) (**28**)	1.0	343	D
$TpRe(CO)(MeIm)(\eta^2$-naphthalene) (**29**)	4.5	343	D
$TpRe(CO)(MeIm)(\eta^2$-benzene) (**30**)	n/a	n/a	n/a
$TpRe(CO)(MeIm)(\eta^2$-anisole) (**31**)	3.0	293	D
$TpRe(CO)(MeIm)(\eta^2$-1-methylpyrrole) (**32**)	6.0	178	D

see Scheme 1.
[a] K_{eq} refers to η^2:η^2 diastereomers (*S*-bound isomer also observed with η^2-bound:*S*-bound ratio = 1.2:1).
[b] K_{eq} refers to η^2:η^2 diastereomers (*S*-bound isomer also observed with η^2-bound:*S*-bound ratio = 5.2:1).

each diastereomer. In all cases, the aromatic complexes bind such that the projection of the bound C=C bond is perpendicular to the Re–CO bond, with the uncoordinated portion of the ring lying over the carbonyl ligand. While a handful of these complexes show a strong preference diastereomer, in general, selectivity is only modest, owing to the lack of significant steric differentiation for the different isomers.

Spin saturation exchange measurements provide a convenient method for analyzing which mechanisms are operative for the interconversion of coordination diastereomers. Fig. 15 shows how spin density is transferred from H1 of a naphthalene complex to either H1′ or H4′ of its coordination diastereomer, depending on the mechanism of isomerization. Likewise, spin density is transferred from H5 of an anisole complex to either H3′ or H5′ of its coordination diastereomer. Using the Forsén–Hoffman relation [30,31], rate constants for each process may be determined, and these data are reported in Table 2. Since the temperature for each

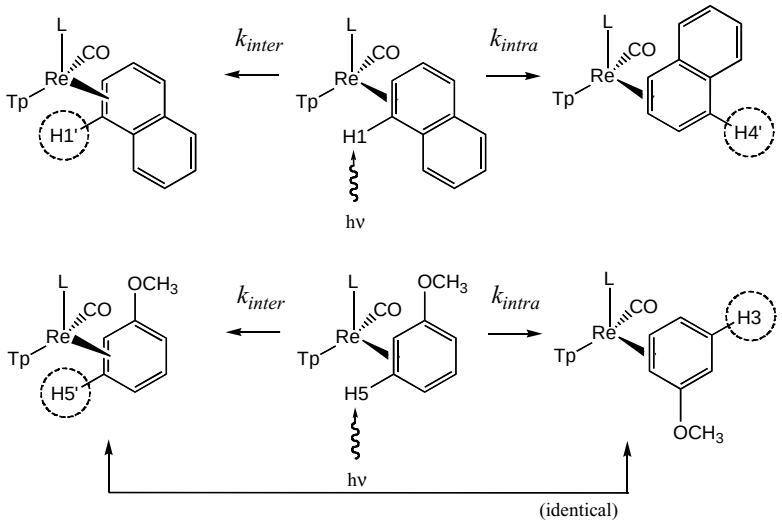

Fig. 15. Spin saturation exchange for intra- and interfacial isomerization of arenes.

Table 2
Observed rates and activation barriers for diastereomeric interconversion of TpRe(CO)(L_D)(η^2-L_{Ar}) systems

Compound	Interfacial migration			Intrafacial migration		
	T_{inter} (K)	$k_{1(inter)} \times 10^{-2}$ (s^{-1})[a]	$\Delta G^{\dagger}_{inter}$ (kcal/mol)[b]	T_{intra} (K)	$k_{1(intra)} \times 10^{-2}$ (s^{-1})[a]	$\Delta G^{\dagger}_{intra}$ (kcal/mol)[b]
TpRe(CO)(^{t}BuNC)(η^2-furan) (**15**)	273	56.2	16.2	273	0.212	18.0
TpRe(CO)(^{t}BuNC)(η^2-2-methylfuran) (**16**)	298	107	17.4			
TpRe(CO)(^{t}BuNC)(η^2-thiophene) (**17**)[c]	273	18.3	16.9	273	17.2	16.9
TpRe(CO)(^{t}BuNC)(η^2-naphthalene) (**18**)		<1	>18.4	273	278	15.4
TpRe(CO)(^{t}BuNC)(η^2-2-methoxynaphthal)(**19**)		<1	>20.8			
TpRe(CO)(^{t}BuNC)(η^2-1,8-dimethylnaphth)(**20**)	293	54.6	17.5			
TpRe(CO)(PMe_3)(η^2-furan) (**21**)	323	91.8	19.0	323	1.37	21.7
TpRe(CO)(PMe_3)(η^2-thiophene) (**22**)[d]	323	98.8	19.0	323	19.4	20.0
TpRe(CO)(PMe_3)(η^2-naphthalene) (**23**)	n/a	n/a	n/a	n/a	n/a	n/a
TpRe(CO)(py)(η^2-furan) (**24**)	323	5.01	20.9		<1	>21.9
TpRe(CO)(py)(η^2-thiophene) (**25**)	323	4.44	21.0	323	1.12	21.9
TpRe(CO)(py)(η^2-naphthalene) (**26**)		<1	>21.9	323	12.4	20.3
TpRe(CO)(MeIm)(η^2-furan) (**27**)	343	2.18	22.8		<1	>23.3
TpRe(CO)(MeIm)(η^2-thiophene) (**28**)	343	1.53	23.0		<1	>23.3
TpRe(CO)(MeIm)(η^2-naphthalene) (**29**)		<1	>23.3	343	3.41	22.5
TpRe(CO)(MeIm)(η^2-benzene) (**30**)[e]				233	1.14	14.5
TpRe(CO)(MeIm)(η^2-anisole) (**31**)[f]	293	20.0	18.1	293	84.8	17.2
TpRe(CO)(MeIm)(η^2-1-methylpyrrole) (**32**)[g]				213	65.5	10.6

[a] k_1 is the rate of migration from the minor diastereomer to the major diastereomer as defined in Table 1; errors in rates are estimated to be ±5%.
[b] Errors in $\Delta G^{\ddagger}$ are estimated to be ±0.3 kcal/mol.
[c] Observed spin saturation exchange with *S*-bound isomer.
[d] Observed no spin saturation exchange with *S*-bound isomer.
[e] Refers to migration from 1,2-η^2 to 2,3-η^2 isomer.
[f] Refers to migration from 2,3-η^2 to 5,6-η^2 isomer.
[g] Measured using coalescence data of bound protons.

system must be adjusted such that the rate falls in the correct timescale to make the measurement, rate constants are converted to free energies of activation in order for meaningful comparisons to be made. In all cases where arene is equal to naphthalene, the intrafacial isomerization dominates with free energies of activation ranging from 15.4 to 22.5 kcal/mol, depending of the nature of the chiral auxiliary L. However, the interfacial isomerization is not inaccessible for naphthalene complexes. When 1,8-dimethylnaphthalene is examined, a system in which the intrafacial isomerization is expected to be endothermic, the interfacial isomerization is measured to be 17.5 kcal/mol. For the complex TpRe(CO)(MeIm)(anisole), *both* inter- and intrafacial isomerization mechanisms are operative, the intrafacial mechanism occurring approximately four times that of the interfacial isomerization at 20 °C. This observation is consistent with what was originally speculated for osmium(II).

For the heterocycle complexes, three outcomes are possible [32]. In addition to a intrafacial or interfacial isomerization mechanism resulting in the interconversion of isomers (Fig. 16), the involvement of the heteroatom is possible. In the latter scenario, a rapid rotation/inversion of the η^1-heteroatom complex is expected to result in an equal transfer of spin density from H4 of the original species to H3′ and H4′ of the new isomer. As Table 2 indicates, the furan complexes explored (L = BuNC, PMe_3, py, and MeIm) all have interfacial isomerizations that are more rapid than the intrafacial isomerization, but both mechanisms are operative with free energies ranging from 16.2 to 23 kcal/mol [32]. In contrast, for 1-methylpyrrole, the intrafacial isomerization dominates (10.6 kcal/mol, where L = MeIm). Where the heterocycle is thiophene, participation of the heteroatom was anticipated, as reported in previous work by Choi and Angelici [33]. The PMe_3 and isonitrile analogs provide an interesting contrast in the participation of the heteroatom. Both complexes exhibit an *S*-bound isomer in their ^{1}H NMR spectra at room temperature. Yet these systems show a striking difference in inter- and intrafacial isomerization rates. Rates for inter- and intrafacial isomerization are identical for the isonitrile complex (**17**) while for the phosphine analog (**22**), they differ by a factor of five. The isonitrile thiophene complex exhibits spin saturation exchange between the η^2 and *S*-bound isomers, whereas the phosphine derivative shows spin saturation exchange *only* between the η^2-thiophene isomers. This observation indicates that for this complex at least, *interconversion between the two η^2 coordination diastereomers does not occur via an S-bound intermediate*, neither for the inter- or intrafacial process.

Data from Table 2 (**15**–**32**) highlight important relationships between the rates of coordination isomerization and the electronic properties of the metal [32]. Fig. 17 shows the strong correlation between both reduction

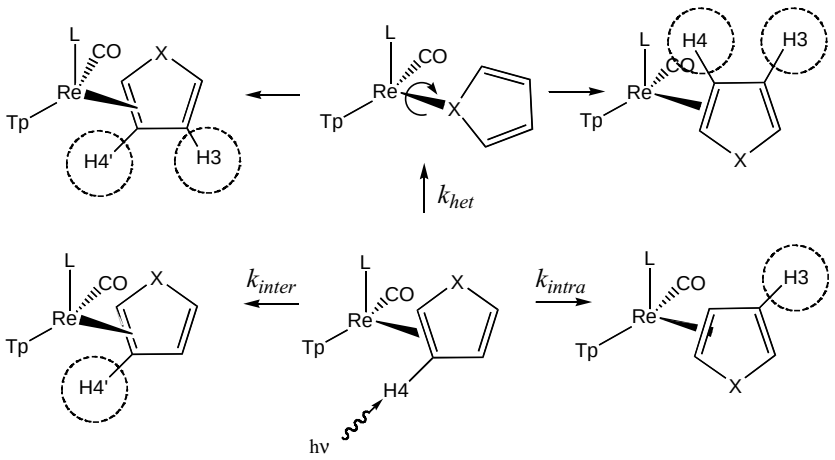

Fig. 16. Spin saturation exchange for intra- and interfacial isomerization of heterocycles.

potential (approximated by anodic peak potential) and the carbonyl stretching frequency and the intermolecular rate of isomerization for the rhenium η^2-furan complexes. This feature, which also holds for intrafacial isomerizations and for aromatic ligand displacement rates [32], is thought to reflect the differing stability of the ground states as a result of the degree of backbonding (see Fig. 4). As a reference point, the interfacial isomerization rate was also measured for a simple alkene. For the complex TpRe(CO)(PMe_3) (*cis*-2,5-dideuterofuran) (**33**) this rate is 30 kcal/mol (c.f. furan complex $\Delta G^{\ddagger} = 19$ kcal/mol) [32].

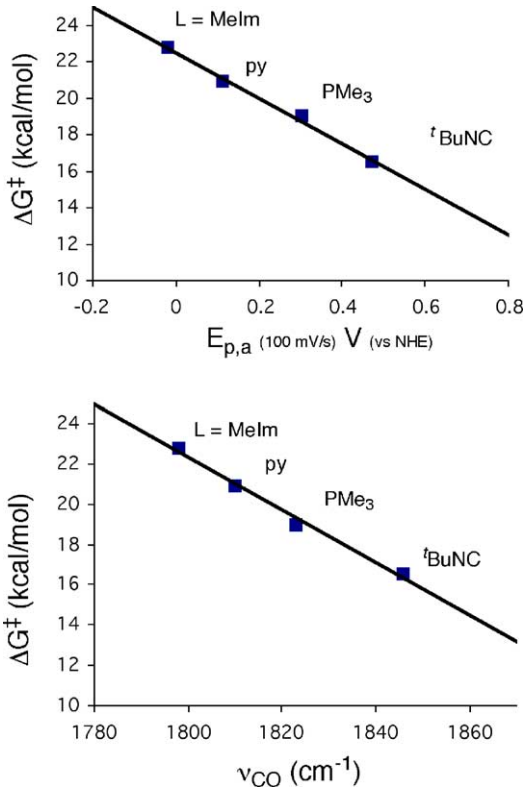

Fig. 17. Correlation of interfacial isomerization free energy of activation and CO stretching frequency and reduction potential for TpRe(CO)L(η^2-furan).

Although not directly related to the coordination isomerizations described in this text, rotation around the metal aromatic ligand bond also causes broadening, particularly in the case of the complex TpRe(CO)(py)(naphthalene) (**26**) [29]. This dynamic process was not investigated to the detail that the coordination isomerizations were, but a series of ethene complexes of the form TpRe(CO)(L)(ethene) was examined by variable temperature NMR [34], and rotational barriers were found to range from 8.0 kcal/mol (BuNC) to 12.5 kcal/mol (MeIm) for the set of four auxiliary ligands discussed above. As with the coordination isomerizations, the more electron-rich the metal fragment, the higher the barrier [34].

3.2. Molybdenum(0) and tungsten(0) nitrosyl complexes

Recently, we have discovered that for the complexes of the form TpRe(CO)(L)(aromatic), replacement of the rhenium by a Group VI metal (Mo, W) can be accomplished, provided that the CO is also replaced with the stronger π acid NO^+ (Fig. 18) [35,36].

Comparing these tungsten and molybdenum complexes with their rhenium analogs, the rates for inter- and intrafacial coordination isomerization are very similar [37]. The TpMo(NO)(MeIm) system seems to most closely correspond to the TpRe(CO)(py) system in terms of isomerization rates and binding ability. The TpW(NO)(PMe_3) system, on the other hand, more closely resembles the TpRe(CO)(MeIm) system. For example, the anisole complex **37** has intrafacial isomerization and ligand displacement rates, isomer selectivities, and reduction potentials that are almost identical to the rhenium–anisole complex (**31**) at room temperature. In one important aspect, dynamics for the tungsten and rhenium systems are very different, however, The ligand–metal rotational barrier for **36** is about 10 kcal higher than for the rhenium analog (**21**).

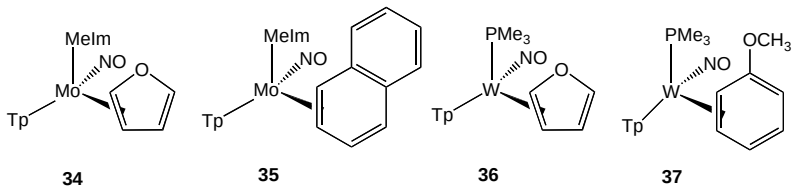

Fig. 18. Group VI complexes of η^2-aromatic complexes.

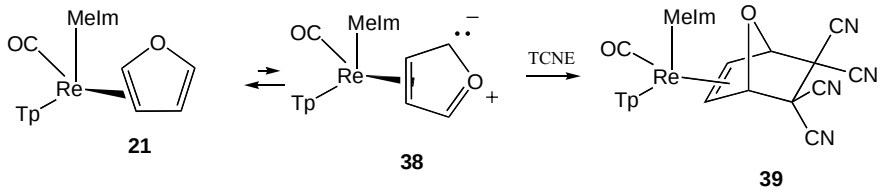

Fig. 19. Evidence for a carbonyl ylide intermediate (a 3,4-η^2-furan).

Correspondingly, rotamers of TpW(NO)(PMe_3)(furan) (**36**) are separable by chromatography [38]. While much less is known about these tungsten systems, in several cases we have conclusively identified conformational isomers in which the uncoordinated portion of the aromatic ring extends into quadrants B and C (see Fig. 14).

Recall that the osmium pyrrole complexes could be trapped in the unusual 3,4-η^2 azomethine ylide coordination diastereomer using an electron-deficient alkene. In a similar manner, rhenium and tungsten furan complexes are shown to be in equilibrium with an oxomethine ylide (carbonyl ylide). For example, when the complex TpRe(CO)(PMe_3)(furan) (**21**) is treated with TCNE, the 7-oxanorbornene **39** is generated in 73% yield (Fig. 19).

3.3. Solid-state induced control of kinetically unstable stereoisomers (SICKUS)

While exploring the stereochemistry of protonation of anisole, we were plagued with seemingly inconsistent results. The observation of high stereocontrol only at very low temperatures lead us to believe at first that the complex TpRe(CO)(BuIm)(anisole) (**41**), which existed as a 3:1 mixture of coordination stereoisomers, showed a high kinetic preference for protonation of a single stereoisomer. Repeating this result was problematic until we realized that the addition order was more important than the temperature. When a solid sample of **41** was added to an acidic solution, only one isomer of the 2*H*-anisolium complex ***H*−41A** was formed. However, if the anisole complex was dissolved first, then treated with acid, a diastereomer ratio of anisolium complexes similar to that of its precursor was obtained (***H*-41A**:***H*-41B** = 2:1). This suggested that in the solid state, only one coordination diastereomer (**41A**) was present, even though the solid was precipitated in nearly quantitative yield directly from a 3:1 (***H*-41A**:***H*-41B**) stereoisomer mixture (Fig. 20).

Under a variety of conditions, observations comparable to those described above were made for a series of {TpM(π-acid)(L)} complexes of prochiral arenes (Table 3), all of which were prepared by their precipitation from a solution containing equilibrium ratios of coordination diastereomers. Once TpM(π-acid)(L)(η^2-arene) complexes are protonated, interfacial isomerization becomes sufficiently slow at ambient temperatures such that no conversion is observed over many hours in solution. Evidence of a high degree of homomorphism in the solid state can therefore be observed indirectly, by trapping the arene complexes as their conjugate acids, even at ambient temperature. Remarkably, these TpM(π-acid)(L)(η^2-arene) complexes appear to have a uniformly homomorphic solid state, even when samples are prepared by simple precipitation from solution. These solids are often *amorphous* in that they do not show sufficient long-range order to diffract X-rays. Alternatively, crystals can be grown from solution by layering hexanes over a THF or diethyl ether solution. In all cases that we have observed (Table 1), the only coordination isomer present, according to the X-ray structure determination, was the same isomer found in the powder sample prepared from precipitation.

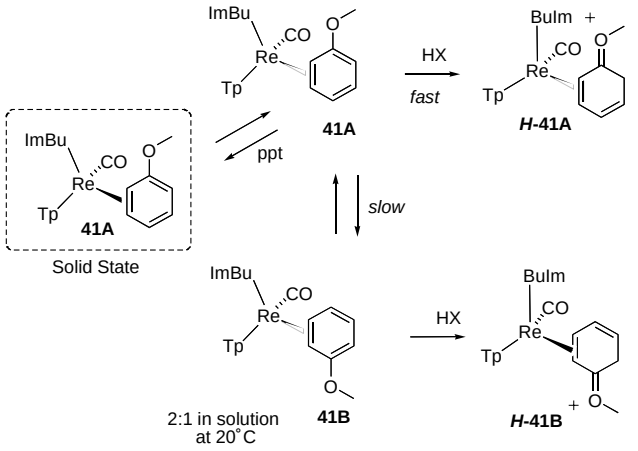

Fig. 20. Crystallization induced asymmetric transfer (CIAT) with a rhenium–anisole complex.

Table 3
Solution equilibrium and solid-state ratios for η^2-arene complex coordination diastereomers

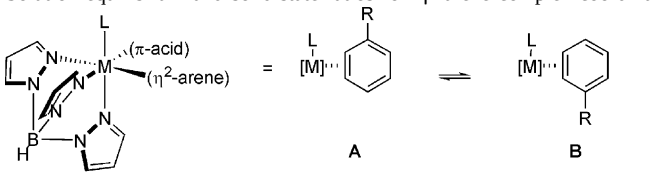

Facial diastereomer designated by orientation of arene substituents with respect to L.

Complex	Equilibrium A:B[a]	Initial A:B[b]	Protonated A:B[c]	Crystal structure	
				Isomer	Space group
[MeImRe]-anisole (**31**)	2:1	2:1[d]	>20:1	A	$P2(1)/n$
[MeImRe]-3-methylanisole (**40**)	2:1	2:1[d]	<1:20	–	–
[MeImRe]-naphthalene (**29**)	4.5:1	>20:1[e]	>20:1	A	$P2(1)/n$
[BuImRe]-anisole (**41**)	2:1	>20:1[f]	>20:1	A	$P-1$ (No. 2)
[BuImRe]-3-methylanisole (**42**)	2:1	12:1[g]	>20:1	A	$P-1$
[BuImRe]-4-methylanisole (**43**)	1:2	1:12[f]	1:6	A	$P-1$
[BuImRe]-naphthalene (**44**)	3.5:1	>20:1[h]	>20:1	–	–
[PyRe]-naphthalene (**26**)	3:1	>20:1[f]	10:1	A	$C2/c$ (#15)
[PMe_3Re]-naphthalene (**23**)	<1:20	<1:20[i]	<1:20	–	–
[MeImMo]-naphthalene (**35**)	4:1	>20:1[f]	>20:1	A	$P2(1)/n$
[PMe_3W]-anisole (**37**)	3.5:1	>20:1[f]	>20:1	A	$P2(1)/c$

[*M*] = {TpM(π-acid)}, [MeImRe] = {TpRe(CO)(MeIm)}, [BuImRe] = {TpRe(CO)(BuIm)}, [PyRe] = {TpRe(CO)(Py)}, [PMe_3Re] = {TpRe(CO)(PMe_3)}, [MeImMo] = {TpMo(NO)(MeIm)}, [PMe_3W] = {TpW(NO)(PMe_3)}.

[a] Ratio of coordination diastereomers observed in equilibrated solutions at ambient temperature.

[b] Highest ratio of coordination diastereomers observed.

[c] Highest ratio of protonated coordination diastereomers observed [32].

[d] Complete solvation could not be effected at low temperature.

[e] Acid-free CD_2Cl_2 at −20 °C.

[f] Acid-free CD_2Cl_2 at −80 °C.

[g] Acetone-d_6 at −60 °C.

[h] Acetone-d_6 at ambient temperature.

[i] Acetonitrile-d_3 at ambient temperature.

Table 3 illustrates how even minor changes in molecular structure can influence the morphology of the solid state. For example, complexes **31** and **40** differ only by the addition of a methyl group at C3 of the anisole ligand, a location well removed from any possible intramolecular steric interaction with the metal complex. As expected, in solution, the A:B ratios are identical. Yet, the dominant diastereomer in the solid state is **A** for anisole, and **B** for 3-methylanisole. Complexes **40** and **42** differ only by the alkyl group attached to the ancillary imidazole ligand. Where L = *N*-methylimidazole (**40**), diastereomer **B** dominates the solid state, while for L = *N*-butylimidazole (**42**), only isomer **A** is present. In solution, the observed A:B ratio is again 2:1 for both complexes. In all, high homomorphism in the solid is observed for three different metals, four different auxiliary ligands, and four different arenes.

4. Controlling the absolute stereochemistry of organic transformations with η^2-aromatic ligands

While a full discussion of the organic reactions that our group has been pursuing with these dearomatization agents is beyond the scope this account, below I describe three conceptually different examples of how controlling coordination stereochemistry translates into control of stereochemistry for organic synthesis.

4.1. Arene chiral auxiliaries with pentaammineosmium(II) [20]

As discussed earlier, using a lactate-derived chiral auxiliary for anisole, the metal can be directed to one enantioface of the anisole ring. The key interactions here are a hydrogen bonding interaction between the ester group and the acidic ammine ligands, and a steric interaction in the unfavored isomer between the methyl group of the auxiliary and the ortho proton (see Fig. 6). Whereas, the auxiliary controls the position of the metal, the metal controls the stereochemistry of any subsequent organic reactions. Consider the sequence of reactions shown in Fig. 21. Addition of the acetal dimethoxymethane followed by addition of the silyl ketene acetal MMTP results in the methoxydiene 45 with both electrophile and nucleophile adding to the ring face opposite to metal coordination. Reduction to the alcohol followed by elimination provides the allyl complex 48, which can be treated with various nucleophiles to provide cyclohexene complexes **50** and **52**. Oxidative decomplexation

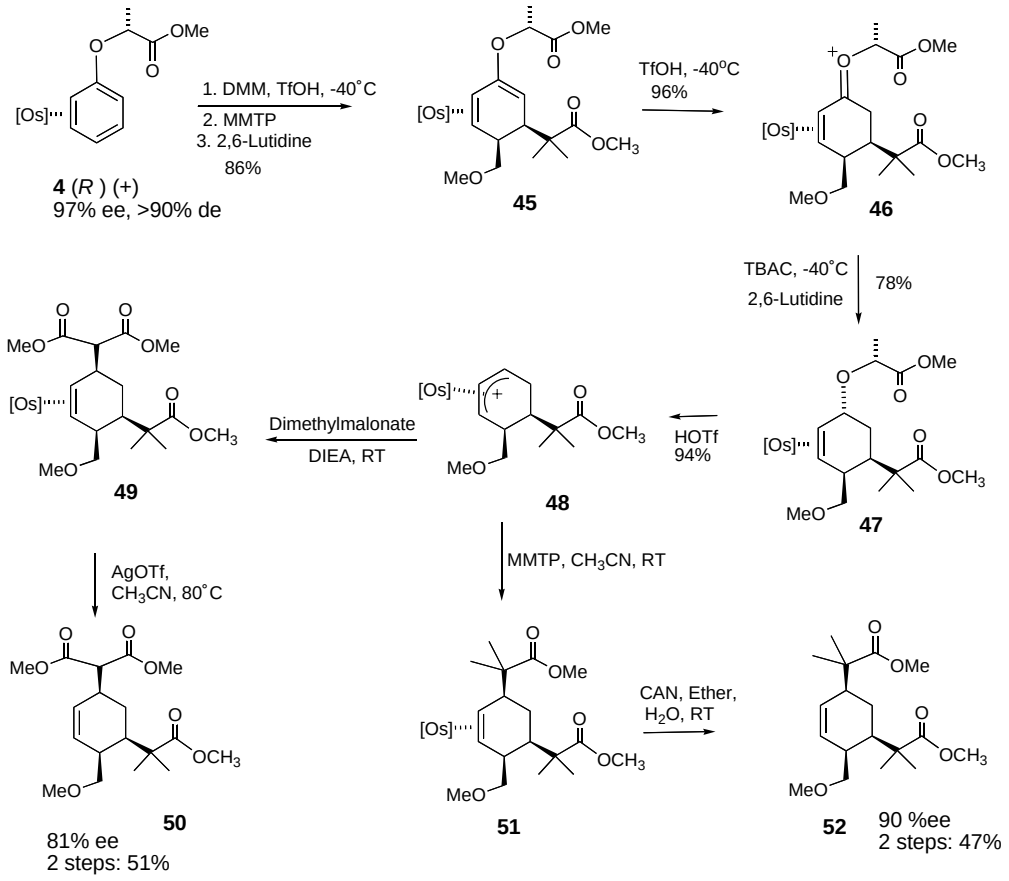

Fig. 21. Formation of enantio-enriched trisubstituted cyclohexenes from anisole.

yields trisubstituted cyclohexenes with three new stereocenters isolated in 80–90% ee and >95% de (average yield per step 83%).

4.2. Influence of the stereogenic metal center [39]

When η^2-furan complexes are treated with an electrophile, addition to the uncoordinated beta carbon results in a 3*H*-furanium species, which can undergo C–O scission to form a metallacyclopropene intermediate [40,41]. If a Michael acceptor is used as the electrophile, the resulting enolate can attack the metallacyclopropene or "vinyl cation" to form a cyclopentene complex with creation of several new stereocenters [39]. The complex TpRe(CO)(MeIm)(η^2-2,5-dimethylfuran) exists in equilibrium as a single coordination diastereomer as a result of the steric interaction between the methyl group off of the bound carbon and quadrant C (see Fig. 14). Thus, when a resolved form of this complex (**54**) is combined with Michael acceptors, highly enantio-enriched cyclopentenes (e.g., **56**) can be recovered (Fig. 22).

4.3. Utilization of SICKUS in organic synthesis [42]

To demonstrate the utility of using SICKUS (Section 3.3) in controlling stereochemistry of η^2-arene complexes,

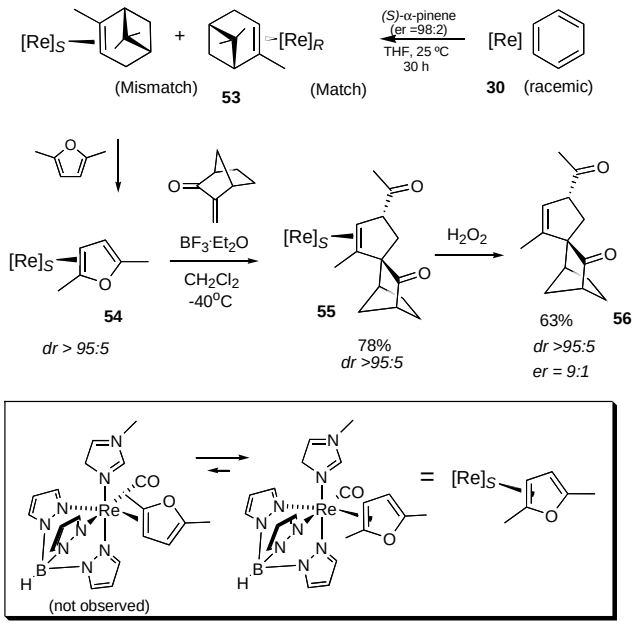

Fig. 22. Cyclopentannulation with a resolved rhenium η^2-furan complex.

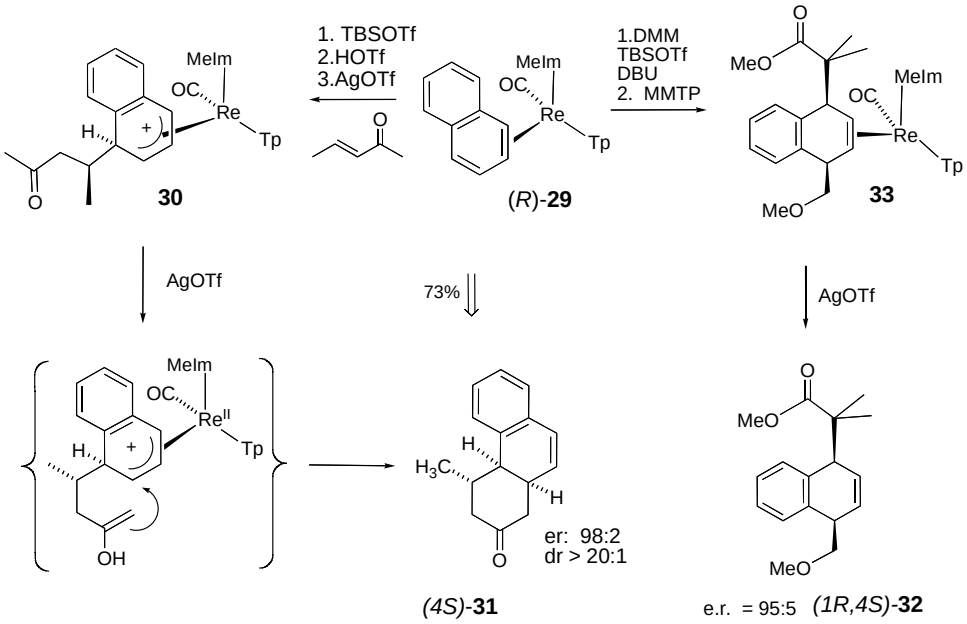

Fig. 23. CIAT applied to the synthesis of a phenanthrenone ring system.

we applied this method to two reaction sequences utilizing the naphthalene complex TpRe(CO)(MeIm)(3,4-η^2-naphthalene) (**29**). Samples of this complex were resolved with 97% ee α-pinene (er = 99:1) [43], and were incorporated in both a 1,4-tandem addition and a Michael–Aldol cyclization sequence, as shown in Fig. 23. In each case, the complex was exposed to the electrophile under conditions such that the chemical reaction was anticipated to occur faster than interconversion of the coordination diastereomers. Final organic products were obtained with er's of 95:5 and 98:2, respectively. When the identical reaction sequences were performed by allowing the naphthalene complex to dissolve in solution *prior to addition of the electrophile*, the er's of the recovered products were 3:1 and 8:1, respectively, ratios similar to the 4.5:1 ratio found for **9** in solution at equilibrium [42].

5. Concluding remarks

Through their dihapto coordination to a transition metal, arenes undergo controlled addition reactions with good stereocontrol relative to the position of the metal. The metal can readily undergo inter- and intrafacial linkage isomerizations, and if this process can be controlled using chiral auxiliaries, stereogenic metal centers, or crystallization-induced asymmetric transfer, enantio-enriched organic compounds can be realized. While the chemistry of η^2-arenes has evolved considerably since its inception in the Taube labs, its bedrock is a strong metal-to-ligand backbonding interaction, a theme that has pervaded Taube's research for much of his brilliant career.

Acknowledgements

Acknowledgement is made to the donors of The Petroleum Research Fund, administered by the ACS, for partial support of this research (ACS-PRF#36638-AC1). This work was also supported by the NSF (CHE0111558 and 9974875) and the NIH (NIGMS: R01-GM49236).

References

[1] A.R. Pape, K.P. Kaliappan, E.P. Kündig, Chem. Rev. 100 (2000) 2917.
[2] M.F. Semmelhack, in: E.W. Abel, F.G.A. Stone, G. Wilkinson (Eds.), Comprehensive Organometallic Chemistry II, vol. 12, Pergamon Press, Oxford, UK, 1995, pp. 979.
[3] W.E. Silverthorn, Adv. Organomet. Chem. 13 (1975) 47.
[4] L.S. Hegedus (Ed.), Transition Metals in the Synthesis of Complex Organic Molecules, University Science Books, Sausalito, 1999 pp.
[5] E.L. Muetterties, J.R. Bleeke, E.J. Wucherer, Chem. Rev. 82 (1982) 499.
[6] P.A. Lay, R.H. Magnuson, J. Sen, H. Taube, J. Am. Chem. Soc. 104 (1982) 7658.
[7] W.D. Harman, H. Taube, Inorg. Chem. 26 (1987) 2917.
[8] W.D. Harman, Chem. Rev. 97 (1997) 1953.
[9] H. Taube, Comments Inorg. Chem. 1 (1981) 17.
[10] R.E. Rundle, J.H. Goring, J. Am. Chem. Soc. 72 (1950) 5337.
[11] R.W. Turner, E.L. Amma, J. Am. Chem. Soc. 85 (1963) 4046.
[12] P.L. Smith, M.D. Chordia, W.D. Harman, Tetrahedron 57 (2001) 8203.
[13] W.D. Harman, H. Taube, J. Am. Chem. Soc. 109 (1987) 1883.
[14] W.D. Harman, M. Sekine, H. Taube, J. Am. Chem. Soc. 110 (1988) 5725.
[15] F.A. Cotton, Acc. Chem. Res. 1 (1968) 257.
[16] W.D. Jones, F.J. Feher, J. Am. Chem. Soc. 104 (1982) 4240.
[17] W.D. Jones, L. Dong, A.W. Myers, Organometallics 14 (1995) 855.

[18] J.R. Sweet, W.A.G. Graham, Organometallics 2 (1983) 135.
[19] C.O. Trindle, G. Sacks, W.D. Harman, Int. J. Quantum Chem. 92 (2003) 457.
[20] M.D.H. Chordia, W.D. Harman, J. Am. Chem. Soc. 122 (2000) 2725.
[21] M.D.H. Chordia, W.D. Harman, J. Am. Chem. Soc. 120 (1998) 5637.
[22] T.S. Peng, J.A. Gladysz, J. Am. Chem. Soc. 114 (1992) 4174.
[23] M.D. Winemiller, B.A. Kelsch, M. Sabat, W.D. Harman, Organometallics 16 (1997) 3672.
[24] R. Cordone, W.D. Harman, H. Taube, J. Am. Chem. Soc. 111 (1989) 2896.
[25] R. Cordone, W.D. Harman, H. Taube, J. Am. Chem. Soc. 111 (1989) 5969.
[26] W.H. Myers, J.I. Koontz, W.D. Harman, J. Am. Chem. Soc. 114 (1992) 5684.
[27] J. Gonzalez, J.I. Koontz, W.H. Myers, L.M. Hodges, M. Sabat, K.R. Nilsson, L.K. Neely, W.D. Harman, J. Am. Chem. Soc. 117 (1995) 3405.
[28] M.T. Valahovic, Doctoral Dissertation, University of Virginia, 2002.
[29] S.H. Meiere, B.C. Brooks, T.B. Gunnoe, E.H. Carrig, M. Sabat, W.D. Harman, Organometallics 20 (2001) 3661.
[30] S. Forsén, R.A. Hoffman, J. Chem. Phys. 19 (1963) 2892.
[31] S. Forsén, R.A. Hoffman, J. Chem. Phys. 40 (1964) 1189.
[32] B.C. Brooks, S.H. Meiere, L.A. Friedman, E.H. Carrig, T.B. Gunnoe, W.D. Harman, J. Am. Chem. Soc. 123 (2001) 3541.
[33] M.-G. Choi, R.J. Angelici, J. Am. Chem. Soc. 111 (1989) 8753.
[34] L.A. Friedman, S.H. Meiere, B.C. Brooks, W.D. Harman, Organometallics 20 (2001) 1699.
[35] P. Graham, S.H. Meiere, M. Sabat, W.D. Harman, Organometallics 22 (2003) 4364.
[36] S.H. Meiere, J.M. Keane, T.B. Gunnoe, M. Sabat, W.D. Harman, J. Am. Chem. Soc. 125 (2003) 2024.
[37] For the TpMo(NO)(MeIm)(naphthalene) complex **35**, the free energy of activation for interfacial isomerization is 21.2 kcal/mol (20 °C). C. Mocella, D. Delafuente, J.M. Keane, G. Warmer, L. Freiedman, M. Sabat, W.D. Harman, Organometallics, in press.
[38] K. Bassett, F. You, W.D. Harman, unpublished results.
[39] L.A. Friedman, F. You, M. Sabat, W.D. Harman, J. Am. Chem. Soc. 125 (2003) 14980.
[40] H.H. Chen, W.D. Harman, J. Am. Chem. Soc. 118 (1996) 5672.
[41] H. Chen, R. Liu, W.H. Myers, W.D. Harman, J. Am. Chem. Soc. 120 (1998) 509.
[42] J.M. Keane, F. Ding, M. Sabat, W.D. Harman, J. Am. Chem. Soc., in press.
[43] S.H. Meiere, M.T. Valahovic, W.D. Harman, J. Am. Chem. Soc. 124 (2002) 15099.